CFD Simulation Of The Zircaloy/Steam Oxidation In The CANDU Fuel Channel Experiments: CS28-2

Hyoung Tae Kim, Bo Wook Rhee and Joo Hwan Park
Korea Atomic Energy Research Institute,
Dukjin-Dong, Yusong-Gu, Daejon 305-303, Korea

Abstract

Oxidation of zircaloy cladding exposed to a high temperature steam is an important phenomenon for the safety analysis of CANDU reactors during a postulated loss-of-coolant accident (LOCA), since this zircaloy/steam reaction is highly exothermic and results in a hydrogen production. The CS28-2 high temperature experiment represents this accident scenario well. As a part of a CFD (Computational Fluid Dynamics) simulation for the CS28-2 experiment, a zircaloy/steam reaction model is implemented into a commercial CFD code, CFX-10, because the present version of the CFX-10 code does not include a surface reaction model.
First, the present oxidation model for the CFX-10 code is validated against the model correlations implemented into the CFX-10 code, and then applied to the simulation of the CS28-2 experiment. The CFX predictions of a temperature rise in the heater rods are compared with the temperature measurements to confirm the validity of the oxidation heat release calculated by the present model. Furthermore, the prediction of a hydrogen generation as a byproduct of the oxidation reaction is validated against the amount of the collected hydrogen in the experiment.

1. Introduction

The decay energy in fuel rods during a post-blowdown period of a CANDU reactor heats up the zircaloy (Zr) of the fuel rods and the pressure tubes. It also ignites a chemical reaction between Zr and steam (H_2O). This is an exothermic reaction, i.e., it results in the production of heat as well as a hydrogen gas (H_2) as follows:

$$Zr + 2H_2O = ZrO_2 + 2H_2 + 586\ kJ \quad (1)$$

If this heat removal is insufficient, the resultant high temperatures and a rapid heating may cause a failure of the fuel channel integrity. Therefore, it is important to have a thorough understanding of a high-temperature fuel channel behavior and the effectiveness of a moderator as a heat sink to demonstrate the safety of CANDU reactors during postulated accidents.
To understand a fuel channel behavior during a LOCA condition, the CHAN thermal Chemical Experiments [1] had been performed at the Whiteshell Laboratories in Canada. The CS28-2 experiment [2,3] is one of the experiments for the simulation of a high-temperature steam cooling condition in a full scale horizontal fuel channel with a 28-element fuel bundle which is electrically heated.
The temperature transient in the 28-element bundle is affected by the amount of electrical power and the exothermal heat generated in this bundle during a CS28-2 test. As a part of a Computational Fluid Dynamics (CFD) simulation of the CS28-2 high temperature experiment for this accident analysis, two zircaloy/steam reaction models based on a parabolic rate law are implemented in a commercial CFD code (CFX-10) [4] through a user FORTRAN.
This paper is about preliminary work for a transient simulation of the CS28-2 experiment: two zircaloy/steam oxidation models used in the CANDU fuel channel codes such as CAHENA [5] and CHAN-II [6] are implemented into the CFX-10 code through a user FORTRAN since the CFX-10 code does not include a surface reaction module. The zircaloy/steam reaction models by

Urbanic et al. [7] and Baker et al. [8] are considered for these CFX-10 applications. These models are based on the parabolic/Arrhenius behavior of the isothermal oxidation experiments: their correlations (Urbanic-Heidrick and Baker-Just correlations) are expressed by the reaction rate equations in form of parabolic oxidation laws.
The CFX-10 code with the present surface oxidation model can calculate the extra heat energy in the solid domain (zircaloy) and the hydrogen mass source in the fluid domain (steam). This oxidation model for a CFX-10 code application is validated by benchmark tests and experimental results. First, it is confirmed that the CFX-10 calculations reproduce the results of each empirical correlation in the simple benchmark tests well. Then a validation against the CS28-2 experiment is performed. The CFX-10 predictions of a temperature transient in the heater rods of the CS28-2 experiment are compared with the experimental results to investigate the validity of the oxidation heat release calculated by the present model. And the CFX-10 prediction of a hydrogen generation as a byproduct of the oxidation reaction is validated against the amount of the hydrogen accumulated in the exit of the test section.

2. The zircaloy/steam reaction model for the CFX-10 code application

2.1 Reaction rate constant

It is generally accepted that the mechanism which governs this reaction is the diffusion of oxygen anions through the anion-deficient ZrO_2 lattice [1]. The reaction rate can be described by a parabolic expression of the form

$$\omega^2 = K_p t\,, \tag{2}$$

where ω is a measure of the extent of the reaction (i.e., weight of zirconium reacted per unit area), t is the reaction time, and K_p is the parabolic reaction rate constant. The K_p is related to the temperature by an expression of the form

$$K_p = A\exp\left(-\frac{E}{RT}\right). \tag{3}$$

where A is a pre-exponential factor, E is the reaction activity energy, R is the ideal gas constant, and T is the temperature of the oxidization layer (K).
Several investigations have been made to determine K_p as a function of the temperature. One of these works, the oxidation model by Urbanic et al. [7] is used for the default model of the CATHENA code [8]. The resulting K_p is given by the following correlations:

$$K_p = 29.6\exp\left(-\frac{16820}{T}\right) \qquad \text{for } T \le 1850\ \text{K} \tag{4}$$

$$K_p = 87.9\exp\left(-\frac{16610}{T}\right) \qquad \text{for } T > 1850\ \text{K} \tag{5}$$

Substituting $\rho_z \times \delta$ for ω in the Eq. (2) and by a differentiating with respect to time [3], we can obtain:

$$\frac{d\delta}{dt} = \frac{K_p}{2\rho_z^2\delta}, \tag{6}$$

where δ is the thickness of the zircaloy consumed during an oxidation and ρ_z is the density of the zircaloy.

2.2 Application to the CFX-10 code

For the CFX-10 code application, the rate of a heat generation (Q) as a result of the zircaloy/steam reaction at high temperatures is expressed as:

$$Q = CA_S \frac{d\delta}{dt}. \tag{7}$$

where C is the heat generation per unit volume of Zr (4.22×10^{10}) and A_s is the surface area of the reaction. This reaction requires that there be a Zr and a ZrO_2 region. The Zr-steam oxidation model starts to be applied when a solid component's temperature reaches 827°C.

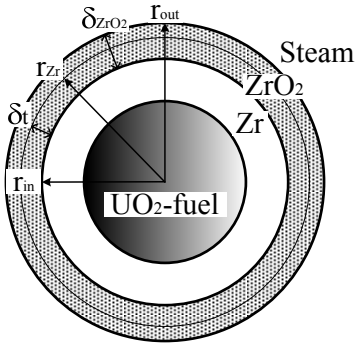

Figure 1 Configuration of the growth of the ZrO_2 layer in a fuel pin.

To correctly simulate the oxidation reaction and the thermal response of the oxidizing layer, the growth of the ZrO_2 layer must be traced. For a fuel pin as shown in **Fig. 1**, let r_{out} and r_{in} be the instantaneous radii of the ZrO_2-steam interface and the ZrO_2-Zr interface, respectively. The original (no-oxidation: $\delta = 0$) outer radius of the fuel element is r_{Zr}. When zircaloy is consumed by an oxidation, r_{in} moves inward. At the same time, r_{out} moves outward as a result of the volume expansion caused by converting Zr to ZrO_2. The thickness of the zirconium consumed up to time *t* is obtained by integration of Eq. (7) to give:

$$\delta_t = \left(\delta_{t-\Delta t}^2 + \Delta t \cdot \frac{K_p}{\rho_z^2} \right)^{1/2}. \tag{8}$$

where $\delta_{t-\Delta t}$ is the thickness of the zirconium consumed up to time $t-\Delta t$ and Δt is the current time step size.
Then the hydrogen generation rate, H_{out} (mole/s) is

$$H_{out} = P\, A_s \left(\delta_t - \delta_{t-\Delta t} \right), \tag{9}$$

where, P is a constant (1.436×10^5).

2.3 CFX user Fortran for the oxidation model

The oxidation model described in the previous section is implemented into the CFX-10 code. For this purpose, a User CFX Expression Language (CEL) Function which uses a user subroutine for the

oxidation model of the CFX-10 code is created. Then this subroutine is compiled and the library file required by the CFX-10 solver is created.
When creating a User CEL Function, we need some variables to be available for use in the CEL expressions.

Table 1 CEL variables used in a User CEL Function

Name	Units	Meaning
T	K	Temperature
ctstep	-	Current time step
dtstep	S	Time step interval
mf	-	Mass fraction
t	S	Simulation time

3. Validation of the CFX oxidation model

3.1 Benchmark test

3.1.1 Set up of the benchmark problem

In the benchmark problem, a constant steam flow is introduced into the annulus between the cylinder of the zircaloy (outer radius: 0.00765 m) and the surrounding tube (inner radius: 0.0215 m) and the flow length is 0.2 m. The temperature of the zircaloy surface is assumed to be uniform as a temperature boundary condition. The configuration of the benchmark test is shown in **Fig. 2**.

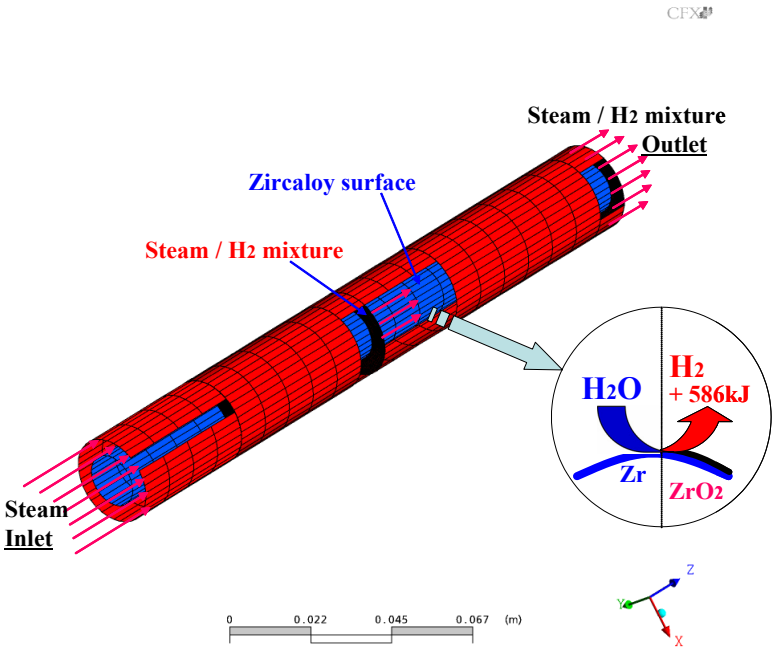

Figure 2 Schematic view of benchmark test.

For the CFX-10 calculations a hexagonal mesh is used and the total number of elements is 11,760. The solid domain for the zircaloy surface and the fluid domain for the steam/hydrogen mixture are modeled in the CFX-Pre. The Urbanic-Heidrick correlation is used for the benchmark calculation of the mass and energy sources in the domain interface between the

zircaloy and steam/hydrogen mixture. Because this correlation has a transition at a temperature of 1850 K, the temperature boundary conditions on the zircaloy surface are divided into two groups: one for below and one for above this temperature.
The initial and boundary conditions for the benchmark test are shown in **Table 2**. The benchmark problems with a total of 6 cases are calculated for 30 sec of a simulation time.

Table 2 Initial and boundary conditions for the benchmark test

Type	**Parameter**	**Group1**	**Group2**
Initial condition	Oxidation thickness, δ_t (m)	1.0×10^{-6}	1.0×10^{-4}
Boundary condition	Steam inlet flow (mole/m^2-s)*	1.7318	
	zircaloy surface temperature (K)	1273 1373 1473	1873 1973 2073

* for the zircaloy surface area: 9.6130×10^{-3} m^2

3.1.2 Benchmark test results

The release of hydrogen simulated by the CFX-10 code is visualized in **Fig. 3**.
The hydrogen mole fraction is circumferentially symmetric, because the composition of the steam/hydrogen mixture and the zircaloy surface temperature are uniform along the circumferential direction. As a mixture of steam and hydrogen flows downward along a zircaloy tube, the hydrogen product is accumulated and its mole fraction is increased. This result is visualized in the longitudinal view in **Fig. 4**.
The H_2 mole fraction calculated from the ratio of the hydrogen production rate (mole/sec) to the steam inlet flow rate (mole/sec) is compared with the result from the CFX-Post (area-averaged value of the variable: H2.Molar Fraction) as shown in **Fig. 5**. The CFX-10 prediction of the H_2 mole fraction reveals a close agreement with the calculation result by the oxidation correlation. As the reaction time increases, the mole fraction at the exit is decreased due to the characteristics of the parabolic reaction rate.
The calculations of the heat flux on the zircaloy surface are compared in **Fig. 6**. Because of the similarity of the mass (hydrogen) and energy (exothermal heat) productions by the oxidation reaction, the results in **Fig. 6** are similar to those in **Fig. 5**.

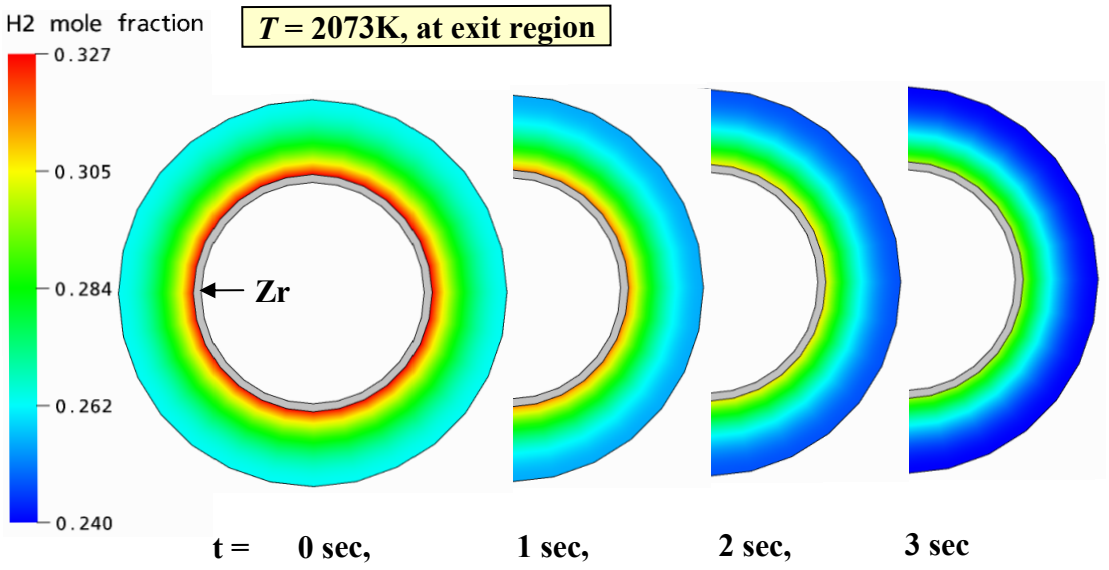

Figure 3 Benchmark test: distribution of H_2 mole fraction.

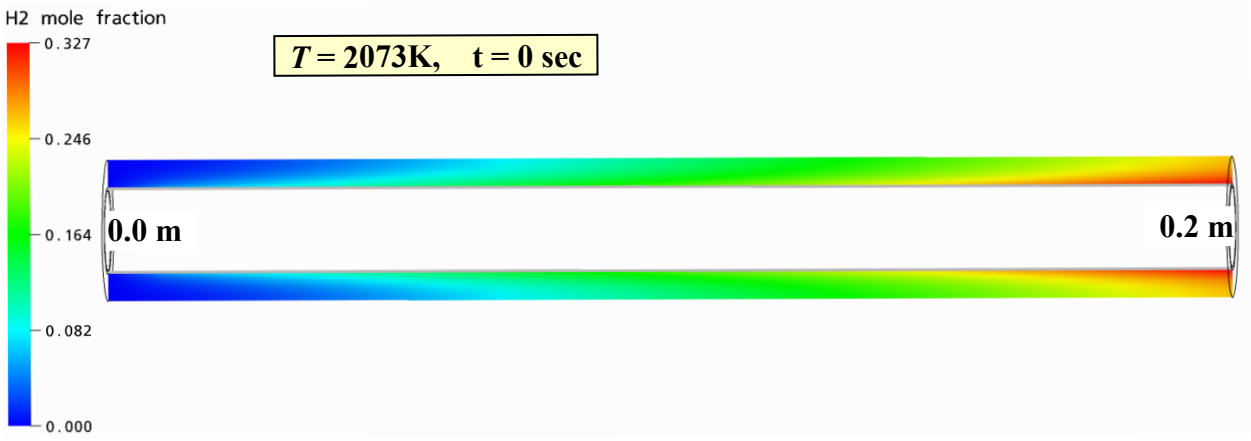

Figure 4 Benchmark test: H_2 mole fraction vs. oxidation length.

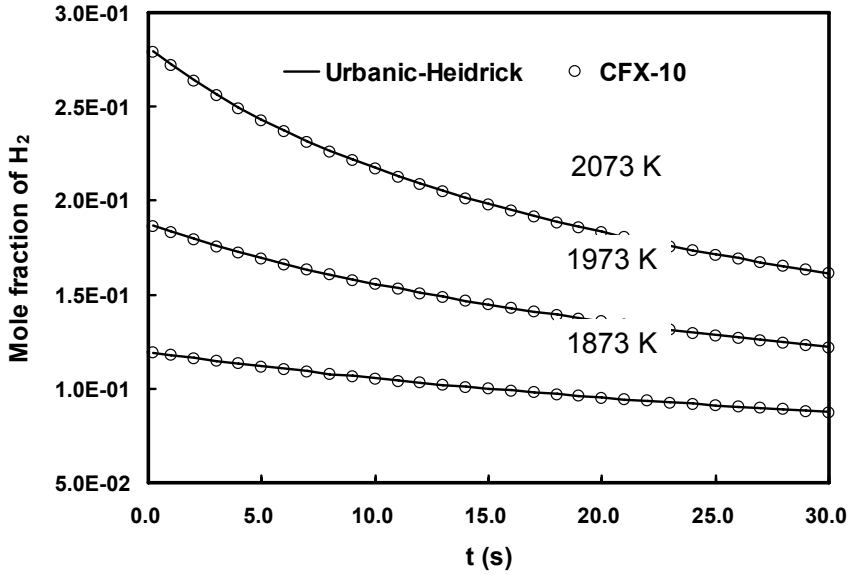

Figure 5 Benchmark test: H_2 mole fraction vs. oxidation time.

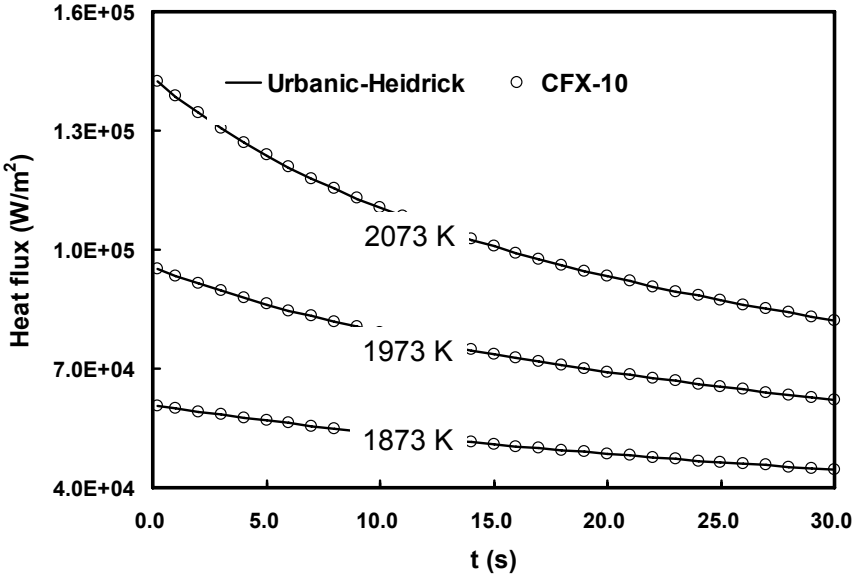

Figure 6 Benchmark test: oxidation heat vs. oxidation time.

3.2 Validation against the CS28-2 experiment

3.2.1 Overview of the CS28-2 experiment

Fig. 7 illustrates the test apparatus of the CS28-2 experiment. A superheated steam at about 700℃ enters the test section from a steam super-heater. In the test, the 28-element bundle raises the temperature of the steam and zircaloy surfaces to temperatures sufficient to cause the zircaloy and steam to react. This reaction produces hydrogen gas and energy which further raises the surface temperatures and increases the reaction rate. The steam and hydrogen gas mixture left the test section and flows into the condenser where the steam was condensed. The hydrogen gas flow was measured by a mass flow meter and vented to the atmosphere.
The procedure for the CS28-2 experiment consists of a low power phase (steady-state condition) and a high power phase (transient condition). At the initial steady-state, the heater power was 10 kW, and the ratios of the pin power were 1.111, 0.894, and 0.755, for the outer, middle, and inner rings, respectively as shown in **Fig. 8**. The transient test started at about 530 sec and its power was raised up to 145 kW and the electric power was turned off at 887 sec.

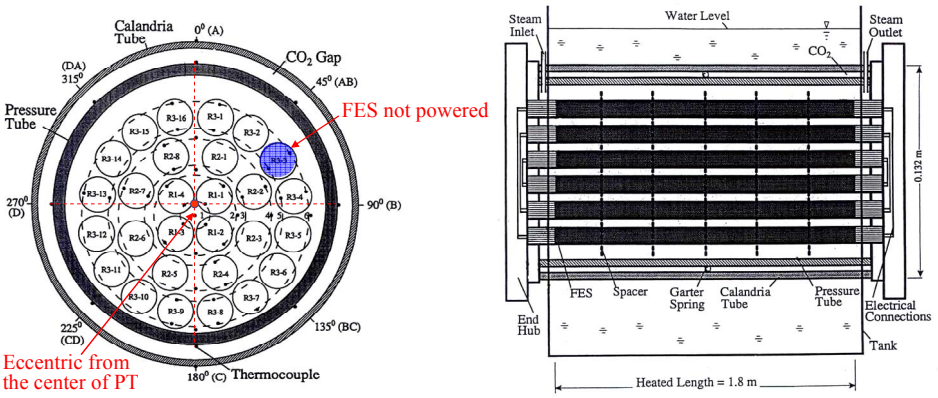

(a) cross sectional view (b) longitudinal view

Figure 7 Schematic diagram of the CS28-2 test.

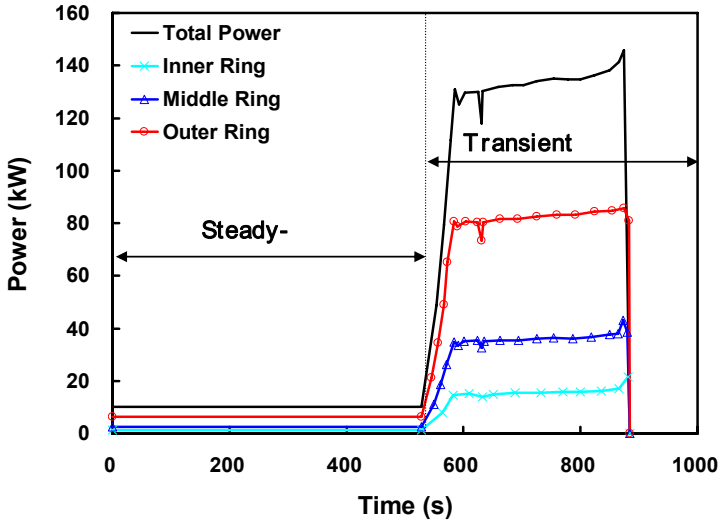

Figure 8 Electric power to the heaters of the CS28-2 experiment.

3.2.2 CFX-10 modelling of the CS28-2

The fluid domains consist of the super-heated steam in the pressure tube and the CO_2 gas in the annulus between the pressure tube and the calandria tube. The solid domains consist of three heater rod walls (including graphite, Al_2O_3, and zircaloy domains), the pressure tube wall, and the calandria wall. The modeling of a pool surrounding the calandria tube is simplified by using a temperature boundary condition (40℃) on the outer surface of the calandria tube.

The grid of the CS28-2 test section is generated by using the ICEM CFD [9] software. A two-dimensional mesh for the cross section of the test section is generated and extruded along the longitudinal direction to obtain a three-dimensional mesh for the test section. The number of nodes with a longitudinal direction (for 1.8 m of an axial length) is 30 by an extrusion of the two-dimensional mesh.

As a turbulence model of the CFX-10 code, the k-ε turbulence model uses the scalable wall-function approach to improve its robustness and accuracy when the near-wall mesh is very fine. The scalable wall functions allow for a solution for arbitrarily fine near wall grids, which is a significant improvement over the standard wall functions. **Fig. 9** shows the results of the grid generation with a refined mesh density near the wall boundaries. The number of elements used is 764,901.

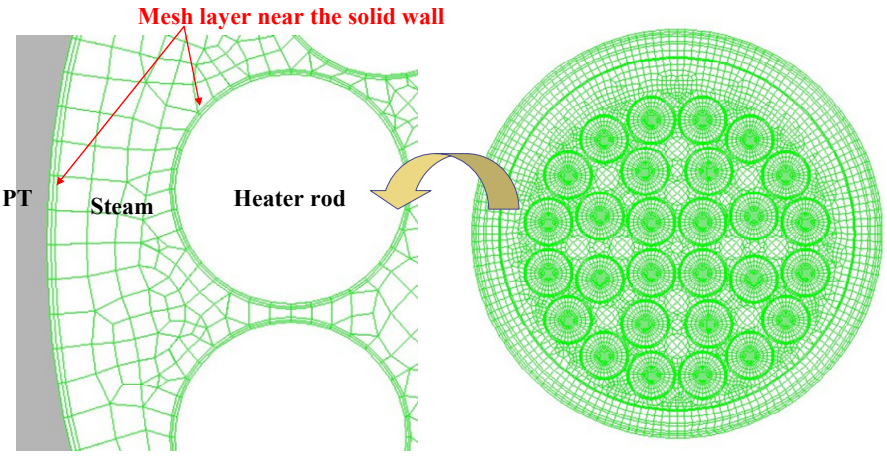

Figure 9 Grid of the CS28-2 test section for the CFX-10 simulation.

3.2.3 Simulation results

According to the present validation procedure, the sensitivity studies include CFX-10 simulations with and without alternative oxidation correlations of Urbanic-Heidrick and Baker-Just. **Fig. 10** shows a comparison of simulated and measured hydrogen production. We can see in **Fig. 10** that results obtained with the Urbanic-Heidrick correlation agreed well with the measured values regarding the total amount of hydrogen produced, although the beginning of a hydrogen production is earlier for the CFX-10 calculations than the measurement. The hydrogen production rate, estimated from the slope of the plot in **Fig. 10**, increases rapidly during a temperature escalation (just before the electric power is turned off about at 900 sec). During this period, the production rate predicted by the Urbanic-Heidrick correlation shows a closer agreement with the measurement. However, a systematic over-prediction of the hydrogen production is predicted when using the Baker-Just correlation over the whole time range. Furthermore, the CFX-10 simulation with the Baker-Just correlation ended abnormally after a too sharp temperature escalation as shown in **Fig. 11**, where one of the sheath temperatures measured in the inner ring are compared with the CFX-10

results. **Fig. 12** shows comparisons of the temperatures on the pressure tube between the measured data and the CFX-10 results. The CFX-10 simulations with the Urbanic-Heidrick correlation for various measurement points in **Figs. 11** and **12** show a close agreement with the experimental results, while the simulations with the Baker-Just correlation overestimate them. The simulations without the oxidation model cannot consider the oxidation heating and underestimate the temperature transients including the peak temperatures of the CS28-2 experiment.
Therefore, it is concluded that an application of the proper oxidation model to the CFX-10 code is essential for a simulation of the CS28-2 experiment and the CFX-10 code with the Urbanic-Heidrick option successfully predicts a temperature transient of the CS28-2 experiment.

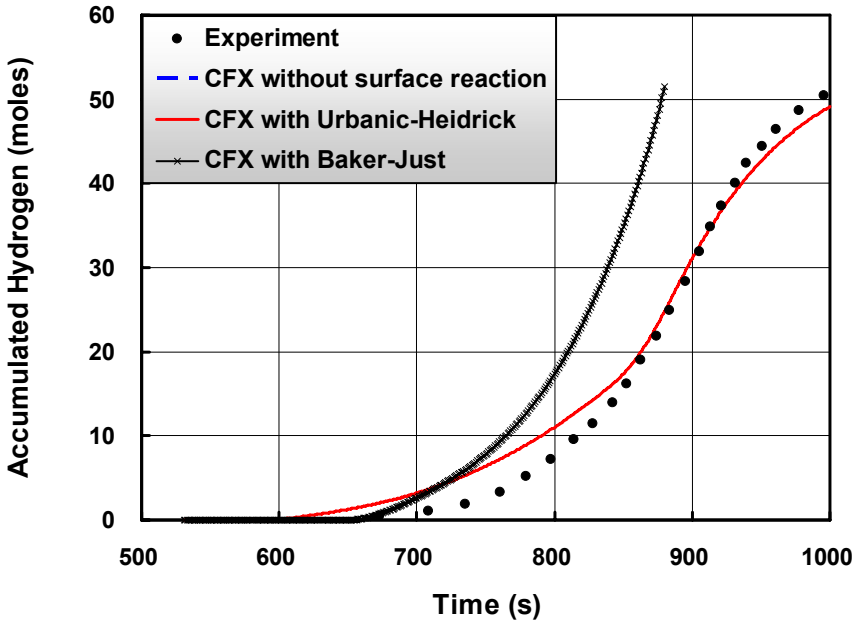

Figure 10 CS28-2 simulation: cumulative H_2 production.

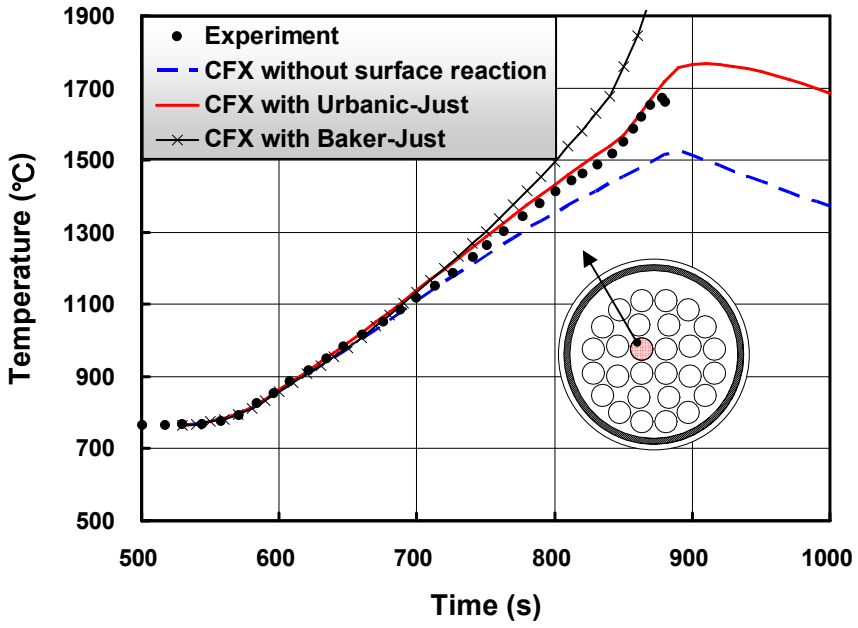

Figure 11 CS28-2 simulation: sheath temperature (R1-4) at 1575 mm from the inlet.

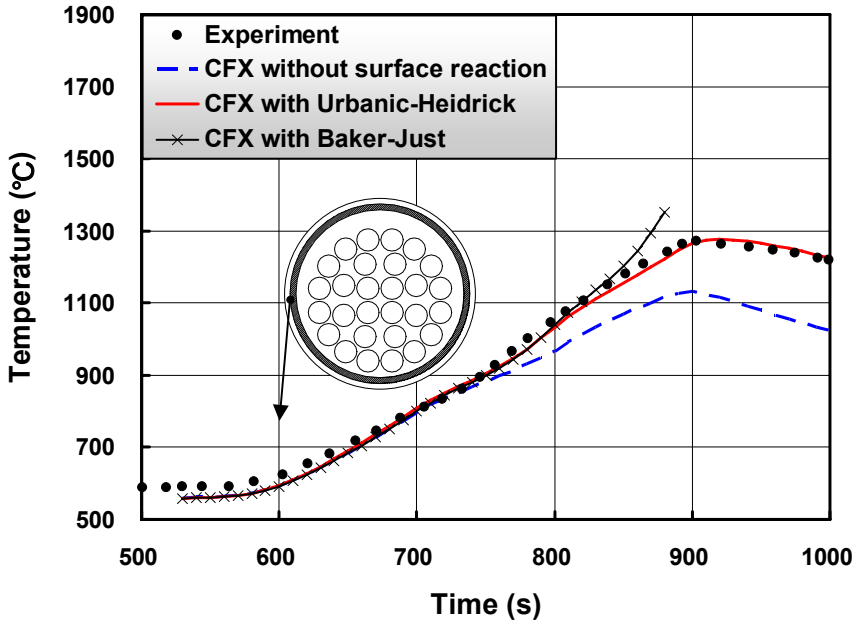

Figure 12 CS28-2 simulation: pressure tube temperature at 1575 mm from the inlet.

4. Conclusion

The zircaloy/steam oxidation models for a CFX-10 application were validated by benchmark tests and experimental results. From the present study the following conclusions can be made.

- The benchmark tests were set up to represent the conditions for a validity of the parabolic reaction model such as a constant temperature and unlimited steam. Over various ranges of temperatures the CFX-10 with the oxidation model was shown to reproduce the results by the oxidation correlation well.

- The temperature measurements and the hydrogen production in the CS28-2 experiment were compared with the predictions by the CFX-10. The CFX-10 predictions with the Urbanic-Heidrick correlation showed a close agreement with the experimental results, while the simulations with the Baker-Just correlation overestimate them.

For a future work, the CFX-10 with the present oxidation model will be used for a full transient simulation of the CS28-2 experiment including a sensitivity study of a grid intensity and a validation against other measurement data.

8. References

[1] Sanderson D.B., Haugen K.A., et al., “Out-of-pile fuel channel experiments for severe accident conditions”, *Proc. ANS Int. Topical Mt. on Safety of Thermal Reactors*, Portland, Oregon, July, 1991, pp.92-100

[2] Bayoumi M.H., Muir W.C., "Post-test simulation and analysis of the second full scale CHAN 28-element experiment (Validation of CHAN-II (MOD6) against experiments)", *Proc. 16th Ann. Conf. of Canadian Nuclear Society,* Saskatoon, Canada, June 4-7, 1995

[3] Mills P.J., Sanderson D.B., Haugen K.A., et al., "Twenty-eight-element fuel-channel thermal-chemical experiments", *Proc. 17th Ann. Conf. of Canadian Nuclear Society,* New Brunswick, Canada, June 9-12, 1996

[4] *ANSYS CFX-Solver, Release 10.0: Theory*, ANSYS, Inc., Canonsburg, 2005

[5] Hanna B.N., "CATHENA: A thermalhydraulic code for CANDU analysis", *Journal of Nuclear Engineering and Design*, Vol. **180** (2), 1998, pp.113-131

[6] Lei, Q., Sanderson, D.B., Brown, M.J., and Rosinger, H.E., "Comparison of CHAN-II_WL Predictions with Measurements Made During Seven-Element High Temperature Thermal Chemical Experiments", *Proc. 12th Ann. Conf. of Canadian Nuclear Society*, Saskatoon, SK, Canada, 1991

[7] Urbanic V.F., Heidrick T.R., "High-temperature oxidation of zircaloy-2 and zircaloy-4 in steam", *Journal of Nuclear Materials,* Vol. **75**, 1978, pp.251-261

[8] Baker L., Just L.C., "Studies of metal-water reactions at high temperatures, III: Experimental and theoretical studies of the zirconium-water reaction", ANL-6548, ANL, 1962

[9] *ANSYS ICEM CFD, Release 10.0: Tutorial Manual*, ANSYS, Inc., Canonsburg, 2005